Catalysis Science & Technology

Accepted Manuscript

ROYAL SOCIETY OF CHEMISTRY

www.rsc.org/catalysis

Catalysis Science & Technology RSCPublishing

PAPER

Photocatalytic conversion of carbon dioxide into methanol in reverse fuel cells with tungsten oxide and layered double hydroxide photocatalysts for solar fuel generation

Cite this: DOI: 10.1039/x0xx00000x

Received 00th November 2013,
Accepted 00th ********** 2014

DOI: 10.1039/x0xx00000x

www.rsc.org/

Motoharu Morikawa,[a] Yuta Ogura,[b] Naveed Ahmed,[b] Shogo Kawamura,[b] Gaku Mikami,[b] Seiji Okamoto,[b] and Yasuo Izumi[b,*]

The phenomena of photocatalytic oxidation of water and photocatalytic reduction of CO_2 were combined using reverse photofuel cells, in which the two photocatalysts, WO_3 and layered double hydroxide (LDH), were separated by a polymer electrolyte (PE) film. WO_3 was used for the photooxidation of water, whereas LDH, comprising Zn, Cu, and Ga, was used for the photoreduction of CO_2. For this process, photocatalysts pressed on both sides of the PE film were irradiated by UV–visible light through quartz windows and through the space in carbon electrode plates and a water-repellent carbon paper for both gas flow and light transmission. 45% of the photocatalyst area was irradiated through the windows. The protons and electrons, which were formed on WO_3 under the flow of helium and moisture, transferred to LDH via PE and external circuit, respectively. Methanol was the major product on LDH under the flow of CO_2 and helium. The observed photoreduction rates of CO_2 to methanol accounted for 68%–100% of photocurrents. This supports the effectiveness of the combined photooxidation and photoreduction mechanism as a viable strategy to selectively produce methanol. In addition, we tested reverse photofuel cell-2, which consisted of WO_3 film pressed on C paper and LDH film pressed on Cu foil. The photoelectrodes were immersed in acidic solutions of pH 4, with the PE film distinguishing the two compartments. Both the photoelectrodes were completely irradiated by UV–visible light through the quartz windows. Consequently, the photocurrent from LDH under CO_2 flow to WO_3 under N_2 flow was increased by 2.4–3.4 times in comparison to photofuel cell-1 tested under similar condition. However, major product from LDH was H_2 rather than methanol using photofuel cell-2. The photogenerated electrons in the irradiated area of photocatalysts were obliged to diffuse laterally to the unirradiated area of photocatalysts in contact to C papers in photofuel cell-1. This lateral diffusion reduced the photocatalytic conversion rates of CO_2, despite the advantages of photofuel cell-1 in terms of selective formation and easy separation of gas-phase methanol.

Introduction

Photocatalytic conversion of CO_2 into fuels has emerged as an attractive option,[1] in terms of both reducing the increased concentration of atmospheric CO_2 as well as generating renewable hydrocarbon fuels that can directly be supplied to our present energy infrastructure. Analogous to photosynthesis, the photocatalytic conversion of CO_2 involves (1) photooxidation of water and (2) photoreduction of CO_2 corresponding to photosystem II, and subsequent dark reactions to incorporate CO_2 into carbohydrates utilizing NADPH formed in photosystem I.[2,3]

Thus far, several researchers have reported photocatalytic cells for water oxidation[2] and proton reduction[4–6] by using Pt–WO_3 and Pt–$SrTiO_3$,[7] as well as TiO_2 and Pt–TiO_2 separated by a polymer electrolyte (PE) film.[8] The combination of steps 1 and 2 of the photocatalytic conversion of CO_2 has been realized using metal complexes and enzymatic photocatalysts.[9] To the best of our knowledge, there are no studies reported on the combination of semiconductor photocatalysts for the photocatalytic conversion of CO_2. In principle, the combination of steps 1 and 2 can be regarded as *reverse* fuel cell operation. This process is considered to be a *reverse* mechanism because the products generated by conventional fuel cells, i.e., CO_2 and H_2O, react to form methanol and O_2, which are the reactants in the conventional fuel cell. In fact, the original concept of reaction between CO_2 and H_2O was proposed[10–12] and demonstrated to be a reverse fuel cell operation,[13] rather than a photocatalytic conversion process.

In this paper, we report the fabrication of a polymer electrolyte fuel cell (PEFC; Figure 1) comprising tungsten oxide (WO_3) and layered double hydroxide (LDH) photocatalysts, and a photofuel cell consisting of acid solutions separated by a PE film (Figure 2). In addition, we experimentally demonstrate solar fuel generation,[10,14–17] in

which the photooxidation of water results in the transfer of protons and electrons to form fuel combined with CO_2.

The primary advantage of using photofuel cells is the band potential of two photocatalysts, which is tunable in comparison with the oxidation and reduction potential of reactions independently, by the choice of the elemental composition of semiconductor catalysts. Traditionally, WO_3 has been the catalyst of choice for the photooxidation of water ($E° = 1.23 - 0.0591 \times$ pH V, 298 K), primarily because of the relatively positive band potential.[18] Similarly, LDH is an unusual class of layered materials comprising positively charged cation layer and interlayer anionic species such as CO_3^{2-}.[19] Recently, researchers have demonstrated the photocatalytic conversion of CO_2 into CO and methanol in water[20] or hydrogen[21–23] by using LDHs comprising Ni, In, Zn, Cu, and Ga. From these reports, we chose LDH compounds comprising Zn, Cu, and Ga for the photoreduction of CO_2 in this study.

In addition, the added advantage of using a photofuel cell is that the photocatalysts used are earth-abundant elements and are relatively inexpensive. Furthermore, the products formed as a result of photocatalysis can be readily separated in the gas phase. This is a unique advantage of using a photofuel cell based on PEFC (Figure 1), as reported for electrocatalytic cell separated by Nafion.[24]

Experimental

Synthesis of WO_3 and LDH consisting of Zn, Cu, and Ga

WO_3 was synthesized by the calcination of ammonium paratungstate pentahydrate $(NH_4)^+_{10}(W_{12}O_{41})^{10-}\cdot 5H_2O$ (Aldrich, >99.99%) in air at 973 K for 4 h.

Nitrogen adsorption isotherm measurements were performed at 77 K within the pressure range 1.0–90 kPa in a vacuum system connected to diffusion and rotary pumps (10^{-6} Pa) and equipped with a capacitance manometer (Models CCMT-1000A and GM2001, ULVAC). The Brunauer-Emmett-Teller surface area (SA) was calculated on the basis of eight-point measurements between 10 and 46 kPa ($P/P_0 = 0.10$–0.45) on the adsorption isotherm. The samples were evacuated at 383 K for 2 h before the measurements. The specific SA of WO_3 thus obtained was estimated to be 20 $m^2\ g^{-1}$.

In this study, we synthesized **LDH1** $([Zn_{1.5}Cu_{1.5}Ga(OH)_8]^+_2[Cu(OH)_4]^{2-}\cdot mH_2O$ starting from nitrates of Zn, Cu, and Ga and ammonium tetracholorocupurate dehydrate at pH 8. Details of the experimental procedure adopted for the synthesis of LDH1 have been reported in literature.[22,23] The exact molecular formula of LDH1, as determined by using extended X-ray absorption fine structure analysis, was found to be $Zn_3Cu_3Ga_2(OH)_{13}[(\mu\text{–}O)_3Cu(OH)(H_2O)_2]\cdot mH_2O$, with the dehydration of three water molecules.[21] Furthermore, the specific SA of LDH1 was estimated to be 62 $m^2\ g^{-1}$.

Design of photofuel cell-1

For this process, 95 mg of WO_3 or 45 mg of LDH1 was suspended in 5% of Nafion dispersion solution (DE521, Wako Pure Chemical; 0.2 mL) and 1-propanol (0.1 mL) and separately mounted onto a water-repellent carbon paper (C paper, TGP-H-060H, Chemix) in an area of 4 cm^2. Subsequently, WO_3 mounted onto the C paper was pressed with LDH1 mounted onto the C paper, separated using a PE film (Nafion, NR-212, Dupont) of thickness 50 μm. The layers were pressed using a tabletop press (Model SA-302, Tester Sangyo Co.) by applying a pressure of 2.0 MPa at 393 K for 10 min. Then the C papers on both sides were carefully removed, resulting in the formation of WO_3–Nafion–LDH1 assembly.

The electronic conductivity of WO_3 and LDH1 was improved by mixing WO_3 (95 mg) and LDH1 (45 mg) with a minimum amount of C black (0.2 mg; Vulcan XC72, specific SA 250 $m^2\ g^{-1}$) using a mortar and pestle. Subsequently, WO_3 and LDH1 obtained were pressed together with a Nafion film separator to form WO_3/C–Nafion–LDH1/C assembly, by using the procedure similar to that adopted for the fabrication of WO_3–Nafion–LDH1.

Photofuel cell-1 designed in this study is shown in Figure S1 (Supplementary Information). The prepared WO_3–Nafion–LDH1 assembly was first sandwiched by a water-repellent C paper and then by C electrode plates, both via a serpentine route (the space section for gas flow and window for light; Figure 1A2, A3). Subsequently, this assembly was sandwiched by quartz window plates. It should be noted that the C paper and C plate were fixed in an area of 2.2 cm^2 and the area of serpentine route was 1.8 cm^2 out of the total 4 cm^2 of each quartz window (Figure 1). Therefore, among catalyst area of 4 cm^2, the area of 1.8 cm^2 (45%) was irradiated through serpentine route whereas the area of 2.2 cm^2 (55%) was blocked by C paper and C plate from light (Figure S1).

Photofuel cell-1 offers the advantage of easy separation of gas-phase products, including methanol. However, a disadvantage associated with the design of the photofuel cell is that only 45% of photocatalysts get irradiated.

CO_2 conversion tests using photofuel cell-1

The fabricated photofuel cell-1 was further tested for its CO_2 conversion efficiency. As the first step, all solvents included in the Nafion dispersion solution was removed by flowing N_2 gas at a rate of 100 mL min^{-1} through a water bubbler maintained at 343 K, independently to WO_3 and LDH1 for 10 h. Subsequently, WO_3 in the system was purged with He gas at a rate of 50 mL min^{-1} through the water bubbler at 323 K. CO_2 (3.5%) with the remaining He gas (total 101 kPa) was circulated in glass line at a rate of 450 mL min^{-1} through LDH1 (Figure 1A1).

WO_3 and LDH1 on the Nafion film were irradiated by UV–visible light from a 500-W xenon arc lamp (Ushio, Model SX-UID502XAM) via a two-way quartz fiber light guide of 1 m (San-ei Electric Co., Model 5Φ-2B-1000L) for 10 h (Figure 1B). The distance between fiber light exit and photofuel cell window was maintained as 50 mm. The light intensity on the photocatalyst was 33 mW cm^{-2}. With the onset of irradiation, the photocatalyst temperature reached as high as 315 K.

The gas circulated through LDH1 was analyzed by an inline gas chromatograph equipped with a thermal conductivity detector (GC-TCD; Shimadzu, Model GC-8A), using He as the carrier gas. The columns were packed with Molecular Sieve 13X-S and polyethylene glycol-6000 supported on Flusin P (GL Science). The current between the two electrodes (Figure 1A1, B) was monitored simultaneously.

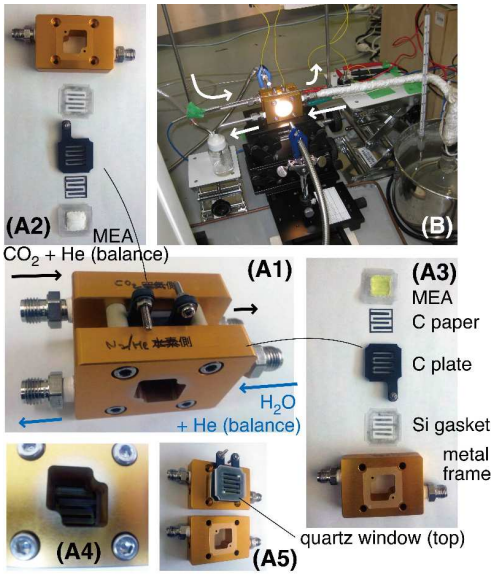

Figure 1. Fabricated photofuel cell-1. The figures show the different components **(A)** and photocatalytic test flowing moisture + He (balance) (front side) and circulating CO_2 + He (balance) (rear side) **(B)**. **A1** depicts photofuel cell-1 at the center of **B**. **A2** and **A3** depict components of photocathode and photoanode, respectively. **A4** is a view of the window of photofuel cell-1. **A5** depicts assembled quartz window, silicon gasket, C electrode plate, C paper, silicon gasket, and WO_3–Nafion–LDH1 assembly.

Design of photofuel cell-2

We also designed photofuel cell-2, as shown in Figure 2. Both photofuel cells were compared for their performance.

For the fabrication of photofuel cell-2, 95 mg of WO_3 was suspended in 5% of Nafion dispersion solution (0.24 mL) and 1-propanol (0.16 mL) and mounted onto a water-repellent C paper in an area of 4 cm^2. WO_3 mounted onto the C paper was then covered with a Kapton film (200H, Dupont) of thickness 50 μm and pressed using a tabletop press (SA-302) by applying a pressure of 2.0 MPa at 393 K for 10 min. Then, the Kapton film was carefully removed to obtain WO_3/C photoelectrode (Figure 2B, right). In a separate process, 45 mg of LDH1 was suspended in 5% of Nafion dispersion solution (0.24 mL) and 1-propanol (0.16 mL) and mounted onto Cu foil (2.3 ×2.5 cm^2) of thickness 30 μm in an area of 4 cm^2. LDH1 mounted onto the Cu foil was then covered with a water-repellent C paper and pressed using a tabletop press (SA-302) by applying a pressure of 2.0 MPa at 393 K for 10 min. Following that, the C paper was carefully removed to obtain LDH1/Cu photoelectrode. In addition, LDH1/Cu photoelectrode was prepared by dispersing LDH1 in 1-propanol (0.4 mL) instead of Nafion dispersion solution in a manner similar to that for LDH1/Cu. LDH1 is sticky and attached to Cu foil even in the absence of Nafion (Figure 2B, left).

CO_2 conversion tests using photofuel cell-2

As the next step, we analyzed the CO_2 conversion performance of photofuel cell-2. For this, the prepared WO_3/C and LDH1/Cu photoelectrodes were immersed in aqueous hydrochloric acid solution (50 mL at each electrode) at pH 4.0, separated by a 50-μm-thick Nafion film at the center of the cell (Figure 2A). Subsequently, N_2 and CO_2 were bubbled at a rate of 50 mL min^{-1} through the sides of WO_3 and LDH1, respectively. Both photocatalysts were irradiated using a 500-W Xe arc lamp via a two-way quartz fiber light guide. The photocatalysts were irradiated from both sides (Figure 2A) for 30 min and kept in the dark for 30 min. The light on/off cycle was repeated five times. The distance between the fiber light exit and the photoelectrode was maintained as 50 mm. The light intensity on the photocatalyst at this position was 33 mW cm^{-2}.

Moreover, smaller photofuel cell-2 was also fabricated (Figure 2C) to make the product concentration relatively higher for the GC analysis. 15 mL of HCl solution was introduced at each electrode. CO_2 was circulated in glass line at a rate of 450 mL min^{-1} through the side of LDH1. The other conditions were similar to that for Figure 2A. The gas circulated through LDH1 was analyzed by the inline GC-TCD (Model GC-9A) using Ar as the carrier gas and also a GC-flame ionization detector (FID; Shimadzu, Model GC-18A) equipped with a capillary column Ultra ALLOY-5 (Frontier Laboratories; inner diameter 250 μm, length 30 m) using He as the carrier gas.

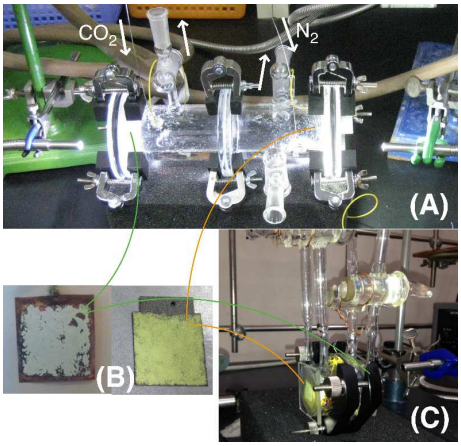

Figure 2. Fabricated photofuel cell-2. The figures show the different components **(A)** and LDH1 mounted onto Cu foil and WO_3 mounted onto water-repellent C paper **(B**, left to right). The smaller cell-2 was also used in which the LDH1 side (right) was circulated with CO_2 gas **(C)**.

Results

CO_2 to methanol conversion in photofuel cell-1

WO_3 on one side of the Nafion film was irradiated with UV–visible light under the flow of He and moisture, while LDH1 on the other side of the Nafion film was irradiated with UV–visible light under the flow of CO_2 (3.5%) (Figure 1B). The main product of the reaction was methanol, whose amount monotonously increased as a function of time irradiated under light (Figure 3, entry a). Other gases generated during the reaction, including CO and methane, were not detected, probably because the amount was below the detection limit of GC. Similarly, H_2 generation could not be monitored, as He was the carrier gas. In this process, the methanol formation rate was estimated to be 0.045 μmol h^{-1} g_{cat}^{-1}, considering that the LDH1 photoelectrode was irradiated through the serpentine route and the effective illumination area is 45% (Figure 1A4).

During the total illumination period of 10 h, the current from LDH1 electrode to WO_3 electrode was stabilized to a constant value of 0.22 μA in 1.6 h (Figure 4a). The current corresponds to an electron flow rate of 0.40 μmol-e^- h^{-1} g_{LDH}^{-1}

from WO_3 to LDH1 (Table 1a). Here 68% of the photocurrent was accounted for the six-electron reduction reaction (6 × 0.045 μmol-CH_3OH h^{-1} g_{cat}^{-1} = 0.27 μmol-e^- h^{-1} g_{cat}^{-1}) from CO_2 to methanol.

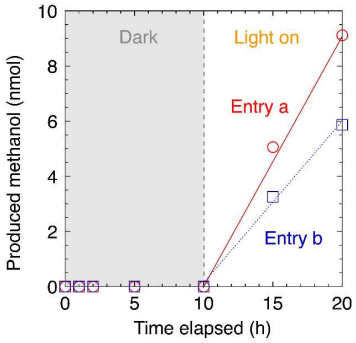

Figure 3. Time evolution of the formation of methanol in photofuel cell-1 consisting of WO_3 and LDH1 (a) and WO_3 and LDH1 mixed with C black (b). The photocatalysts were in dark in 10 h and UV-visible light was irradiated in next 10 h (a, b).

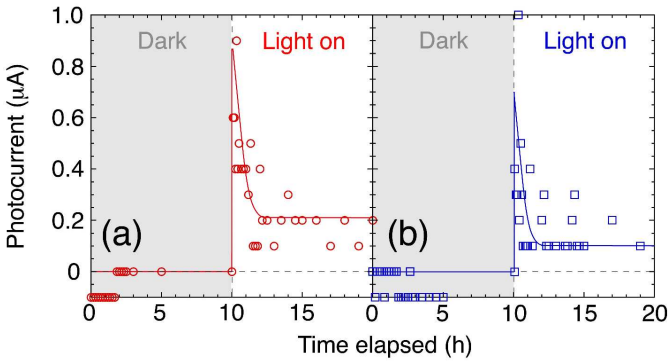

Figure 4. Time evolution of the photocurrent generated during CO_2 conversion tests using photofuel cell-1 consisting of WO_3 and LDH1 (a) and WO_3 and LDH1 both mixed with C black (b). The photocatalysts were in dark in 10 h and UV-vislble light was irradiated in next 10 h (a, b).

Furthermore, we analyzed the effects of mixing C black with the photoelectrodes by comparing the CO_2 conversion performance of the WO_3/C–Nafion–LDH1/C assembly with that of the WO_3–Nafion–LDH1 described above. The CO_2 conversion result of the WO_3/C–Nafion–LDH1/C assembly in photofuel cell is plotted in Figure 3, entry b. As seen from the figure, the methanol formation rate is 0.029 μmol h^{-1} g_{cat}^{-1}. This indicates a reduction in the methanol formation rate by 36% with the addition of C black to LDH1. The lower formation rate should be due to lower light penetration depth into both photocatalyst layers mixed with C rather than the effect of improved electron conductivity by mixing photocatalysts with C. During the test, the photocurrent from LDH electrode to WO_3 electrode stabilized to a constant value of 0.10 μA in 1.6 h (Figure 4b). The constant current corresponds to an electron flow rate of 0.18 μmol-e^- h^{-1} g_{LDH}^{-1} from WO_3/C to LDH1/C (Table 1b). Most of the current accounted for the six-electron reduction reaction (6 × 0.029 μmol-CH_3OH h^{-1} g_{cat}^{-1} = 0.17 μmol h^{-1} g_{cat}^{-1}) from CO_2 to methanol.

The generated photocurrents decreased in initial 1.6 h of irradiation both in Figures 4a and b. In comparison to rather constant formation of methanol (Figure 3), major part of the initial photocurrents would not be due to photocatalysis.

In this study, we performed two blank tests. One blank test was performed at 323 K, which is higher than the maximum temperature (315 K) of kinetic tests irradiated by light, under dark conditions and flow of He and moisture to WO_3 and flow of CO_2 (3.5%) and remaining He to LDH1. The other blank test was performed with light irradiation under the flow of He and moisture to WO_3, and the flow of He to LDH1. For both tests, we could not detect products above the detection limit of GC. The photocurrent was negligible after 2 h of the reaction.

CO_2 to methanol conversion using photofuel cell-2

CO_2 photoconversion performance of photofuel cell-1 was compared with that of photofuel cell-2 containing WO_3 and LDH1 immersed in acid solutions, and fully exposed to light.

For the photofuel cell containing 95 mg of WO_3 and 45 mg of LDH1 separately mounted onto C paper and Cu foil, respectively (Figure 2A, B), the photocurrent gradually increased within 15–20 min of irradiation under UV–visible light and gradually decreased to background level within 10–15 min in the dark (Figure 5a).

The maximum photocurrent from LDH1 electrode to WO_3 electrode was 1.15 μA, as determined from five on/off cycles of light irradiation. The photocurrent corresponded to an electron flow rate of 0.96 μmol h^{-1} g_{LDH}^{-1}, by a factor of 2.4 times greater than that using photofuel cell-1 (Table 1c, a). In this comparison, the electron flow rates were estimated by the area of photocatalyst exposed to light irradiation, e.g., 45% and 100% for photofuel cell-1 and photofuel cell-2, respectively.

In addition, we performed the CO_2 photoconversion test using photofuel cell-2 consisting of WO_3 (95 mg) on C paper and LDH1 (45 mg) on Cu foil, which was prepared without the Nafion dispersion solution. The change in photocurrent during the five on/off cycles of light is depicted in Figure 5b. As seen from the figure, the photocurrent increases gradually under light and decreases gradually to background level in the dark. This trend is very similar to that shown in Figure 5a. However, the maximum photocurrent (1.63 μA) was found to increase by a factor of 1.42 times with the elimination of Nafion in the LDH1 photoelectrode mounted on Cu foil. The photocurrent corresponded to an electron flow rate of 1.36 μmol h^{-1} g_{LDH}^{-1}, which was 3.4 times greater than that using photofuel cell-1 (Table 1d, a).

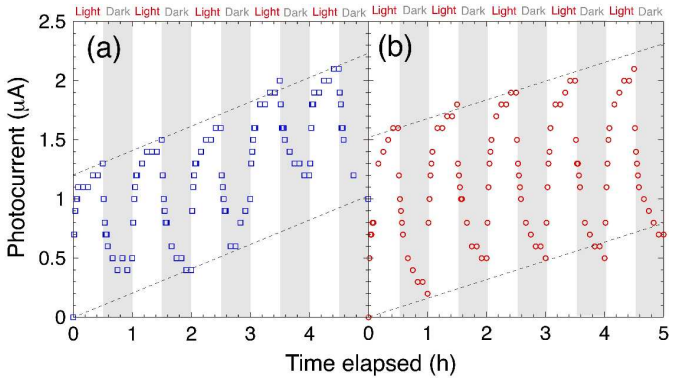

Figure 5. Time evolution of photocurrent generated during CO_2 conversion tests using photofuel cell-2 comprising WO_3 on C paper, prepared using Nafion suspension solution (a, b) and LDH1 on Cu foil, prepared using Nafion suspension solution (a) and prepared using 1-propanol without Nafion (b).

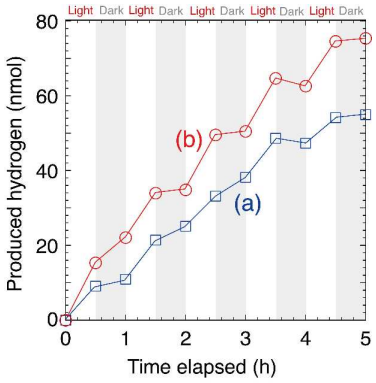

Figure 6. Time evolution of the formation of hydrogen during CO_2 conversion tests using photofuel cell-2 comprising WO_3 on C paper, prepared using Nafion dispersion solution (a, b) and LDH1 on Cu foil, prepared using Nafion suspension solution (a) and prepared using 1-propanol without Nafion (b).

Table 1. Comparison of photocurrents generated during the CO_2 conversion tests using the photofuel cells designed in this study

Entry	Cell type	WO_3[*1] support	LDH1[*2] support	Current (μA)	e^- flow rate (μmol h^{-1} g_{LDH}^{-1})	MeOH or H_2 form rate (μmol h^{-1} g_{LDH}^{-1})
a	Photofuel cell-1	Nafion film	Nafion film	0.22	0.40[*4]	0.045 (MeOH)[*4]
b		Nafion film (C black mixed[*3])	Nafion film (C black mixed[*3])	0.10	0.18[*4]	0.029 (MeOH)[*4]
c	Photofuel cell-2	C paper	Cu foil	1.15	0.96	0.49 (H_2)
d		C paper	Cu foil (No Nafion disp sol used[*5])	1.63	1.36	0.67 (H_2)

[*1] 95 mg. [*2] 45 mg. [*3] 0.2 mg.
[*4] Divided by exposed LDH1 sample to light (45 mg × 0.45).
[*5] LDH1 was dispersed in 1-propanol only and mounted on Cu foil.

Both the gas circulated through LDH1 and the acid solution for LDH1 were analyzed in a separate test using smaller photofuel cell-2 (Figure 2C). The time evolution is depicted in Figure 6. When WO_3 on C paper was purged with N_2 gas and LDH1 on Cu foil was circulated with CO_2, both prepared using a Nafion dispersion solution, hydrogen was a major product from LDH1 (Figure 6, entry a) at a formation rate of 0.49 μmol-H_2 h^{-1} g_{LDH}^{-1}. H_2 formation was also observed in dark cycles. This fact is related to slow decrease of photocurrent in dark cycles (Figure 5a), suggesting diffusion control. Most of the current (0.96 μmol-e^- h^{-1} g_{LDH}^{-1}) accounted for the two-electron reduction reaction (2 × 0.49 μmol-H_2 h^{-1} g_{LDH}^{-1} = 0.98 μmol h^{-1} g_{LDH}^{-1}; Table 1c).

When WO_3 on C paper was purged with N_2 gas and LDH1 on Cu foil was circulated with CO_2, which was prepared without the Nafion dispersion solution, the hydrogen formation by the UV-visible light irradiation became faster, at a rate of 0.67 μmol-H_2 h^{-1} g_{LDH}^{-1} (Figure 6b). Most of the current (1.36 μmol-e^- h^{-1} g_{LDH}^{-1}; Figure 5b) accounted for the two-electron reduction reaction (2 × 0.67 μmol-H_2 h^{-1} g_{LDH}^{-1} = 1.34 μmol h^{-1} g_{LDH}^{-1}; Table 1d).

In both tests of Figure 6a and b, other gases generated during the reaction through LDH1 were not detected above the detection limit of GC-TCD. The acid solution for LDH1 in photofuel cell-2 under the conditions of Figure 6b (Figure 2C) irradiated under UV-visible light for 10 h was analyzed by GC-FID, but methanol was not detected above the detection limit (4.83 pmol in 1.0 μL injection). The detection limit corresponded to formation rate of 0.16 μmol-CH_3OH h^{-1} g_{LDH}^{-1}. Taken the six-electron reduction into account, the detection limit was 0.96 μmol-e^- h^{-1} g_{LDH}^{-1} versus the observed current of 1.36 μmol-e^- h^{-1} g_{LDH}^{-1} (Figure 5b). At least, methanol was not the major product in photofuel cell-2.

Discussion

It is well known that the mechanism underlying the photocatalytic splitting of water using WO_3 under UV irradiation is via the following equation.[25,26]

$$2H_2O \rightarrow O_2 + 4H^+ + 4e^- \qquad (1)$$

In this study, WO_3 exhibited constant oxygen generation upon irradiation by UV–visible light in the presence of sacrificial oxidant (Ag^+).[27] The potentials for photoreduction reactions, e.g., H_2 formation, are beyond the bandgap energy of WO_3.[18] Thus, the protons generated in this process transferred to LDH1 via Nafion film in case of photofuel cell-1, and via the acid solution and Nafion film in case of photofuel cell-2. On the other hand, the electrons generated in this process transferred to LDH1 via external circuit (Scheme 1).

On comparing the photocurrent generated in photofuel cell-1 and photofuel cell-2 with the same types and amounts of photocatalysts, it was observed that photofuel cell-2 generated higher photocurrent. This suggests that the proton diffusion in HCl solutions (pH 4) of photofuel cell-2 (Table 1c, d) is sufficiently high and that the diffusion of proton in 50-μm-thick Nafion film is relatively critical. The conductivity of Nafion film at relative humidity of 10–100% was reported to be 79 mS cm^{-1} based on electrochemical impedance spectroscopy.[28] If the applied voltage was assumed to be 1 V, the conductivity corresponded to proton conductivity on the order of 10^{-5} mol h^{-1} for Nafion film of thickness 50 μm. In contrast, proton diffusion rate in acid solution (pH) can be estimated based on the catalytic rate of diffusion-limited reaction.[29] Hydrogen formation rate from $Fe_2S_2(CO)_4[P(OCH_3)_3]_2$ complex was on the order of 10^{-1} mol h^{-1}. Apparently, proton conduction in Nafion film is more critical compared to that in acid solution, but it is somewhat faster compared to the charge flow in the cells of this study (3.6–61 nmol h^{-1}; Table 1), suggesting rate control primarily by surface reactions.

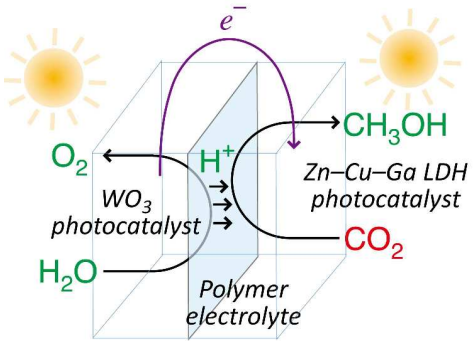

Scheme 1. Schematic illustration of the flow of materials and electrons during photocatalytic CO_2 conversion in reverse photofuel cell-1 consisting of WO_3 and LDH1.

Figures 5a and b show a gradual increase in the background current. This could primarily be attributed to the slow supply of protons to LDH1, leading to a concentration gradient of solutions between WO_3 side and LDH1 side. Alternatively, the pH of the solution in the LDH1 side would have increased with the increase in temperature from 290 to 310 K due to the solubility dependence of CO_2 during the five on/off irradiation cycles. Consequently, to compensate the pH change, the background current might have increased gradually.

Reaction 1 in the presence of catalyst WO_3 is followed by reaction 2 over LDH1.

$$CO_2 + 6H^+ + 6e^- \rightarrow CH_3OH + H_2O \qquad (2)$$

The mechanism underlying reaction 2 seems to be similar to that of reaction 2′, which has been reported for LDH1 and $[Zn_{1.5}Cu_{1.5}Ga(OH)_8]^+{}_2CO_3^{2-}{\cdot}mH_2O$ photocatalysts.[21–23] More specifically, the importance of protonation to one-electron-reduced CO_2 species has been discussed while explaining the formation of formic acid[30] and methane[31] in the presence of TiO_2 and Zn–Ge oxynitride.[32] Specific reaction pathways have been proposed for reaction 2 or reaction 2′, which results in methanol (or CO/methane) via the formation of formaldehyde,[21,23,33] carbene,[33] and glyoxal[33] by multiple protonation steps and electron supply.

$$CO_2 + 3H_2 \rightarrow CH_3OH + H_2O \qquad (2')$$

Similar to the reports for reaction 2′,[21–23] methanol was the major product formed in photofuel cell-1. 68%–100% of electron production/consumption during the steady-state period, between 2 and 10 h, in photofuel cell-1 (Figures 3 and 4) can be attributed to the conversion of CO_2 to methanol. We evaluated the photocatalytic performance starting from H_2O and CO_2 according to the photocurrent from LDH1 to WO_3 electrodes in photofuel cells (Table 1).

The excessive photocurrents observed in the initial 1.6 h in photofuel cell-1 corresponded to 0.022 μmol of electrons (Figures 4a, b). Major part of the initial photocurrents would not be due to photocatalysis. One of the possibilities is that WO_3 proceeded reaction 1 whereas supplied electrons from WO_3 to photocathode were consumed non-catalytically, e.g. the partial reduction of Cu^{II} sites in LDH1 under irradiation. In this study, the amount of Cu used in the cell was 180 μmol. We tried to detect reduced Cu^{I} sites among major Cu^{II} sites in LDH1 used for the test of Figures 5b & 6b by synchrotron Cu K-edge X-ray absorption spectroscopy at KEK-PF & SPring-8.[21,23,34] However, 120 ppm of Cu^{I} at maximum was hard to detect experimentally.

The major generation of hydrogen from the photocathode (LDH1) was directly monitored in photofuel cell-2 (Figure 6). In contrast, part of the photocurrent that was not attributed to the conversion of CO_2 to methanol, which is less than 32% of total photocurrents (Table 1), may be ascribed to the formation of hydrogen in photofuel cell-1. The reduction potential for reaction 2 ($E° = -0.32 - 0.0591 \times$ pH V), in which the term of methanol concentration is negligible compared to proton concentration, is similar to that for reaction 3 ($E° = 0 - 0.0591 \times$ pH V).[35] In the blank test with light irradiation under the flow of He and moisture to WO_3, and He to LDH1 in photofuel cell-1, the photocurrent was negligible, after 2 h of reaction. Thus, H_2 formation was negligible but further photocatalytic reduction to methanol should proceed at the interface of LDH1 and gas (CO_2 & He) in photofuel cell-1 whereas reaction 3 predominantly proceeded at the interface of LDH1 and acid solution of pH 4.0 in photofuel cell-2. The observed clear contrast in selectivity should be because of gaseous CO_2 (3.5%) in photofuel cell-1 (methanol formation) versus the limited solubility of CO_2 in water in photofuel cell-2 (hydrogen formation).

$$2H^+ + 2e^- \rightarrow H_2 \qquad (3)$$

In summary, efficient CO_2 conversion to methanol can be observed over LDH1 in photofuel cell-1, which is analogous to the CO_2 photoconversion to methanol in CO_2 + H_2 mixed gases,[21–23] whereas hydrogen was preferably formed in photofuel cell-2.

Although the major photocatalytic products (methanol or H_2) were different, the electron flow rates in photofuel cell-2 (0.96–1.36 μmol h^{-1} $g_{LDH}{}^{-1}$; Table 1c, d) were observed to be significantly higher, by 2.4–3.4 times, when compared to those in photofuel cell-1 (0.40 μmol h^{-1} $g_{LDH}{}^{-1}$; Table 1a). A reason for this is the longer electron diffusion path from WO_3 layer to C electrode and that from C electrode to LDH1 layer for photofuel cell-1. In particular, the proton transfer in the serpentine area (Figure 1A2–5) should be good, while the electrons separated from holes in the irradiated serpentine area of photocatalysts must laterally diffuse to the unirradiated area of photocatalysts, C paper, and then to the C electrode (anode) connected to the external circuit. For the photocathode, the electron flow from C paper to unirradiated area of LDH1 and then laterally to irradiated serpentine area of LDH1 is needed. For photofuel cell-2, the electrons separated under irradiation easily diffuse into the thin WO_3 photocatalyst vertically to the C paper,[36] and from the C paper vertically to thin LDH1 (Figure 2A, C).

Of the two photofuel cells analyzed in this study, maximum photocurrent was observed (Figure 5b) in photofuel cell-2 consisting of WO_3 and LDH1 photoelectrode on Cu foil prepared without Nafion dispersion solution (Figure 2B). The current was quantitatively in accord with dominant H_2 formation (Figure 6b). Nafion dispersion solution used to mount LDH1 on Cu foil affect negatively to cover the active photoreduction sites (Table 1c, d). Furthermore, X-ray diffraction study of the LDH1 sample indicates that the layered structure of LDH1 is not destroyed during the photoreduction test for 5 h. In spite of this, LDHs as hydroxide-based materials need to be in close contact with Nafion dispersion solution/film would be unstable in longer-term application of photofuel cell-1.

Conclusions and future prospect

A reverse photofuel cell to form O_2 and methanol was designed using WO_3 as the photooxidation catalyst of water and LDH, $Zn_3Cu_3Ga_2(OH)_{13}[(\mu\text{–}O)_3Cu(OH)(H_2O)_2]{\cdot}mH_2O$, as the photoreduction catalyst of CO_2. This cell could be used to enable solar fuel generation if optimum photooxidation/reduction catalysts are chosen independently.

Photofuel cell-1, which was designed on the basis of PEFC, was advantageous in terms of easy separation of methanol gas as the major product. On the other hand, solar fuel generation was limited, especially from the photoelectron flow efficiency viewpoint. The electrons generated in WO_3 by the photooxidation of water were obliged to move laterally to the unirradiated area of WO_3 and then to carbon, and from carbon

to the unirradiated area of LDH1 and then laterally to the irradiated area of LDH1.

Photofuel cell-2, consisting of independent photoelectrodes immersed in acid solution (pH 4), had higher photocurrents, 2.4–3.4 times. However, the reaction on LDH1 directed to H_2 formation and methanol was not found above the detection limit of GC-FID. Future studies are required to improve the photofuel cell-1 and to control the potential of the harder step, i.e., CO_2 photoreduction at photocathode by using sustainable sources such as solar cells.

Acknowledgements

The authors are grateful for the financial support from the Grant-in-Aid for Scientific Research C (Proposal No. 22550117) from Monbukagakusho and the Feasibility Study Stage of A-STEP (Proposal Nos. AS231Z01459C and AS251Z00906L) from the Japan Science and Technology Agency. The X-ray absorption experiments were performed with the approvals of the Photon Factory Proposal Review Committee (Nos. 2011G033 and 2009G552) and the grant of the Priority Program for Disaster-Affected Quantum Beam Facilities (2011A1977, SPring-8 & KEK).

Notes and references

[a] Department of Nanomaterial Science, Graduate School of Advanced Integration Science, Chiba University, Yayoi 1-33, Inage-ku, Chiba 263-8522, Japan.
[b] Department of Chemistry, Graduate School of Science, Chiba University, Yayoi 1-33, Inage-ku, Chiba 263-8522, Japan.
* Corresponding author.
Electronic Supplementary Information (ESI) available: Figure S1. See DOI: 10.1039/b000000x/

1 M. Mikkelsen, M. Jørgensen, and F. C. Krebs, *Energy Environ. Sci.*, 2010, **3**, 43.
2 J. H. Alstrum-Acevedo, M. K. Brennaman, and T. J. Meyer, *Inorg. Chem.*, 2005, **44**, 6802.
3 D. Voet and J. G. Voet, *Biochemistry, 2nd ed.*, pp.626–661 (Chapter 22), Wiley, New York, 1995.
4 K. S. Joya, Y. F. Joya, K. Ocakoglu, and R. van de Krol, *Angew. Chem. Int. Ed.*, 2013, **52**, 10426.
5 K. J. Young, L. A. Martini, R. L. Milot, R. C. Snoeberger III, V. S. Vatista, C. A. Schmuttenmaer, R. H. Crabtree, and G. W. Brudvig, *Coor. Chem. Rev.*, 2012, **256**, 2503.
6 J. Sun, D. K. Zhong, and D. R. Gamelin, *Energy Environ. Sci.*, 2010, **3**, 1252.
7 K. Sayama, K. Mukasa, R. Abe, Y. Abe, and H. Arakawa, *Chem. Commun.*, 2001, **35**, 2416.
8 K. Fujihara, T. Ohno, and M. Matsumura, *J. Chem. Soc. Faraday Trans.*, 1998, **94**, 3705.
9 C. D. Windle and R. N. Perutz, *Coord. Chem. Rev.*, 2012, **256**, 2562.
10 Y. Izumi, *Coord. Chem. Rev.*, 2013, **257**, 171.
11 A. D. Handoko, K. Li, and J. Tang, *Curr. Opinion Chem. Eng.*, 2013, **2**, 200.
12 L. Alibabaei, H. Luo, R. L. House, P. G. Hoertz, R. Lopez, and T. J. Meyer, *J. Mater. Chem. A*, 2013, **1**, 4133.
13 M. Morikawa, N. Ahmed, Y. Ogura, and Y. Izumi, *Appl. Catal. B*, 2012, **117/118**, 317.
14 J. K. Hurst, *Science*, 2010, **328**, 315.
15 H. Gray, *Nat. Chem.*, 2009, **1**, 7.
16 N. S. Lewis and D. G. Nocera, *Proc. Nat. Acad. Sci.*, 2006, **103**, 15729.
17 H. Lv, Y. V. Geletii, C. Zhao, J. W. Vickers, G. Zhu, Z. Luo, J. Song, T. Lian, D. G. Musaev, and C. L. Hill, *Chem. Soc. Rev.*, 2012, **41**, 7572.
18 N. Serpone, P. Maruthanuthu, P. Pichat, E. Pelizzetti, and H. Hidaka, *J. Photochem. Photobio.*, 1995, **85**, 247.
19 F. Li and X. Duan, *Struct. Bond.*, 2006, **119**, 193.
20 K. Teramura, S. Iguchi, Y. Mizuno, T. Shishido, and T. Tanaka, *Angew. Chem. Int. Ed.*, 2012, **51**, 8008.
21 M. Morikawa, N. Ahmed, Y. Yoshida, and Y. Izumi, *Appl. Catal. B*, 2014, **144**, 561.
22 N. Ahmed, M. Morikawa, and Y. Izumi, *Catal. Today*, 2012, **185**, 263.
23 N. Ahmed, Y. Shibata, T. Taniguchi, and Y. Izumi, *J. Catal.*, 2011, **279**, 123.
24 C. Genevese, C. Ampelli, S. Parathoner, and G. Centi, *J. Ener. Chem.*, 2013, **22**, 202.
25 M. G. Walter, E. L. Warren, J. R. McKone, S. W. Boettcher, Q. Mi, E. A. Santori, and N. S. Lewis, *Chem. Rev.,* 2010, **110**, 6446.
26 A. Kudo and Y. Miseki, *Chem. Soc. Rev.*, 2009, **38**, 253.
27 Y. Ogura and Y. Izumi, Japanese Patent, 2012, 223765; 2012, 254796; 2013, 211956; Y. Ogura, S. Okamoto, T. Itoi, Y. Fujishima, Y. Yoshida, and Y. Izumi, *Chem. Comm.*, 2014, DOI: 10.1039/C4CC00194J.
28 R. Yadav and P. S. Fedkiw, *J. Electrochem. Soc.*, 2012, **159**, B340.
29 F. Quentel, G. Passard, and F. Gloaguen, *Chem. Eur. J.*, 2012, **18**, 13473.
30 S. Kaneco, H. Kurimoto, Y. Shimizu, K. Ohta, and T. Mizuno, *Energy*, 1999, **24**, 21.
31 N. M. Dimitrijevic, B. K. Vijayan, O. G. Poluektov, T. Rajh, K. A. Gray, H. He, and P. Zapal, *J. Am. Chem. Soc.*, 2011, **133**, 3964.
32 N. Zhang, S. Ouyang, T. Kako, and J. Ye, *Chem. Commun.*, 2012, **48**, 1269.
33 S. N. Habisreutinger, L. Schmidt-Mende, and J. K. Stolarczyk, *Angew. Chem. Int. Ed.*, 2013, **52**, 7372.
34 Y. Yoshida, Y. Mitani, T. Itoi, and Y. Izumi, *J. Catal.*, 2012, **287**, 190.
35 C. Wang, R. L. Thompson, J. Baltrus, and C. Matranga, *J. Phys. Chem. Lett.*, 2010, **1**, 48.
36 Y. T. Liang, B. K. Vijauyan, K. A. Gray, and M. C. Hersam, *Nano Lett.*, 2011, **11**, 2865.

Photocatalytic conversion of carbon dioxide into methanol in reverse fuel cells with tungsten oxide and layered double hydroxide photocatalysts for solar fuel generation

Motoharu Morikawa, Yuta Ogura, Naveed Ahmed, Shogo Kawamura, Gaku Mikami, Seiji Okamoto, and Yasuo Izumi

Graphical abstract

Photofuel cells comprising WO_3 and layered double hydroxide converted gaseous CO_2 into methanol whereas hydrogen was formed in aqueous phase.